Investing Solar Bifacial Half Cut Single PV Panel for Enriched Power Delivery and System Stability Using Hybrid Approaches

Kante Venkatadurgaprasad[1], Barry Venugopal Reddy[2], Gadiraju Harish Kumar Varma[3], Soumitra Das[4]*

[1]Research Scholar, EEE Department, National Institute of Technology Goa, GOA, INIDA, prasad369durga@gmail.com
[2]Associate Professor, EEE Department, National Institute of Technology Goa, GOA, INIDA, bvenugopal_reddy@nitgoa.ac.in
[3]Assistant Professor, EEE Department, SRKR Engineering College, Bhimavaram, AP, india,gadiraju.harish@gmail.com
[4]Associate Professor, EEE Department, National Institute of Technology Goa, GOA, INIDA, sdas@nitgoa.ac.in.

Abstract: Solar PV modules offer clean, renewable energy, reducing carbon footprint and lowering electricity costs. They provide energy independence and require low maintenance. However, previously adopted techniques like simple MPPT methods often struggled with efficiency under variable irradiance and partial shading conditions. These methods lacked adaptability and precision, leading to suboptimal power extraction and increased reliance on grid electricity. Advanced algorithms and better optimization techniques address these drawbacks by enhancing efficiency and responsiveness. A novel hybrid technique is introduced for maximizing the power output of Solar Bifacial Half cut single PV panels while ensuring consistent power flow within the system. These panels incorporate bifacial technology, capturing sunlight on both their front and rear surfaces, and utilize half-cut solar cells, dividing conventional cells into two smaller ones for increased efficiency and reduced losses, especially in shaded or non-uniform irradiance conditions. The proposed hybrid technique combines the Random Forest Algorithm (RFA) with the Osprey Algorithm (OA), enhancing the prediction accuracy of RFA. In order to maximise PV output power, this combined strategy known as RFA-OA focuses on continuously tracking the Maximum Power Point (MPP). Based on voltage and current parameters, the RFA-OA algorithm specifically calculates the precise duty cycles required for the PV's DC-DC converter under various shading situations. This control method minimises fluctuations in system parameters and outside disturbances to provide the best possible load demand satisfaction. The suggested approach is put into practice in the MATLAB/Simulink environment and contrasted with current practices. It achieves a remarkable maximum output power efficiency of 99.951% for the PV panel, showcasing its efficacy in maximizing power generation while maintaining system stability and reliability.

1 Introduction

Non-renewable energy sources have grown less and less essential in meeting the world's power needs in recent years due to growing concerns about global warming and the efficient use of renewable energy sources (RESs) [1, 2]. The increasing global interest in energy serves as a reminder of the necessity to look into alternative energy sources. The development of renewable energy has proven to be highly beneficial due to the drawbacks of fossil fuels [3-5]. After decades of research, two of the most popular renewable energy sources (RESs) are solar photovoltaic (PV) systems and wind energy systems. Since 1.2 billion people lack access to energy in many developing nations, standalone systems are more economical than connecting power lines to the grid at several places. Hybrid standalone systems provide even more cost-effectiveness by utilizing special energy sources [6–8]. In standalone systems, photovoltaic (PV) technology is notable as the main energy source. While hybrid systems are better in windy areas, hybrid PV-diesel battery systems are particularly useful in areas where winter solar irradiation is significantly lower than summer solar irradiation [9]. Power electronic converter technological developments have lessened the drawbacks of renewable energy systems. Converters use a variety of maximum power tracking techniques, such as buck, boost, and bi-directional converters [10–13]. In solar and wind PV systems, different MPP tracking (MPPT) approaches are used to maximise turbine power output [14]. PV-Wind standalone systems employ MPPT algorithms for converters [15–17]. MPPT approaches come in two: standard and advanced. Conventional methods have trouble in tracking the largest power point under a range of weather conditions. Advanced MPPT approaches are more sophisticated even though they are more efficient than classic procedures [18].Maximizing power extraction in a solar PV module is crucial to enhance overall energy efficiency, reduce dependency

* Corresponding author: prasad369durga@gmail.com

on non-renewable energy sources, and lower electricity costs. Ensuring the PV system operates at its peak power point optimizes the conversion of solar energy into electrical power, thereby maximizing the return on investment for solar installations [19]. Additionally, efficient power extraction contributes to sustainable energy practices, decreases carbon footprint, and supports the transition to a greener energy grid. Overall, it ensures that solar energy systems are both economically viable and environmentally beneficial [20].

2 Objectives of the Research Work

The prediction accuracy of the system is greatly increased when the Random Forest Algorithm (RFA) and Osprey Algorithm (OA) are integrated, especially in situations with dynamic and uneven irradiance. This enhancement allows for more accurate tracking of the MPP of the Solar Bifacial Half-cut single PV panel.

The primary objective of the suggested hybrid technique (RFA-OA) is to optimize the source system's output power.

The MPPT process which is based on RFA-OA, is designed to efficiently handle variations in system parameters and outside disruptions.

The suggested method guarantees the best possible load fulfillment by continuously modifying the PV panel's operational parameters and streamlining the power flow throughout the system.

3 Recent research works: a brief review

The literature has examined a number of methods for controlling power flow and monitoring the MPP in solar PV generating systems. The following is a list of some of these methods:

Ibrahim et al. [21] suggested a hybrid photovoltaic/ wind energy to support and feed the utility grid. Versaci and La Foresta [22] introduced an intuitionistic fuzzy Takagi-Sugeno technique that is optimised for energy management in isolated direct current microgrid systems with solar and wind power. By using an Adaptive MPPT system, Jamadar and Singaram [23] were able to maintain a consistent PV system output and achieve a noteworthy improvement in energy output of about 10.20% when compared to standard MPPT systems. The effect of solar and wind power injection on the small signal stability of an 11 kV power network in Nigeria was assessed by Michael et al. [24]. A hybrid renewable energy system using photovoltaic and wind energy conversion technologies was shown by Elymany et al. [25]. Maka and Chaudhary [26] conducted a model that integrates a photovoltaic system with battery storage in order to boost energy efficiency using solar simulation in the "system advisor model" programme. Endiz [27] approximated the MPPT and fast prototyping of a low-power solar charge controller quickly.

The significance of power flow management and MPP tracking in SPV producing systems is emphasized by the study of recent studies. Variations in load demand as well as climatic information like temperature and radiation provide serious problems for SPV applications, mostly because controlling several energy sources is complicated. Numerous techniques have been used to manage power flow in SPV systems. But although FA adds complexity, FLC needs a lot of data and isn't appropriate for programs that change greatly from past data. These methods are employed for power management, but because more samples are needed, they are more sophisticated. Advanced technology is required for optimum MPP tracking and power flow management in order to tackle these difficulties. Further research in this field is motivated by the paucity of control strategies offered in previous studies to track MPP in SPV systems.

4 Configuration of MPPT system

Fig. 1 illustrates how the Hybrid Renewable Energy System (HRES) is configured to regulate MPPT and Power Flow Management (PFM) in a solar bifacial half-cut single PV panel system with a three-phase AC load. Main and auxiliary sources, such as a single solar PV panel with a bifacial half-cut and a battery acting as an energy storage device, take the place of transient grid conditions. A boost converter is linked to the AC load of the solar bifacial half-cut single PV panel unit to optimise the amount of solar power that is available. In the event that the solar bifacial half-cut single PV panel unit is not there, sustained electricity is provided. The battery uses a simultaneous buck-boost DC transformer to regulate the Energy Storage System (ESS). Every energy unit mentioned before receives electricity from the AC grid through a three-phase Voltage Source Inverter (VSI). The HRES system is linked with the microgrid through Point of Common Coupling (PCC) bus, which also supplies electricity to it through the inverter's DC component. Xc1 stands for the capacitive response itself, resistances R1 and R2, intermediate line inductances L1 and L2, and the parallel X1 and X2 that connect the PCC and inverter. The microgrid's local AC loads' actual and reactive power requirements are represented by the letters PL and QL, respectively. The control outputs are the instantaneous active and reactive power (P1 and Q1), the bus 1 voltage (V1), and the inverter present (Ii). The suggested solution generates control signals that are used to operate the VSI switches using the Pulse Width Modulation (PWM) technique. Mathematical modelling of the solar bifacial half-cut single PV panel is presented in the following section.

5 Modelling of Solar Bifacial Half Cut Single PV Panel System

We use a two-diode model to accurately represent the properties of the solar bifacial half-cut single PV arrays in order to assess the suggested MPPT approach. This modeling technique, especially under low-irradiance situations, not only improves performance accuracy but also cuts down on processing time. The PV cell array is designed by adding a diode connector in parallel to the

current source and calculating the necessary power flow[28, 29]. The circuit in that cell consists of parallel and serial resistors that are connected across the diode. The configuration of photovoltaic cell design is shown in Figure 2. Figures 3 and 4 illustrate the analysis of the power (P-V) and current characteristics (I-V) at different temperatures.

Equations (1) and (2) can be used to evaluate the current flow in circuit "I."

$$I_{PV} - I_d - I_{sh} = I \quad (1)$$

$$I = I_{PV} - I_d - I_s\left[\exp\left(\frac{qR_T}{akT}\right) - 1\right] \quad (2)$$

where I_{PV} specifies PV current, T specifies Diode temperature, I_s specifies leakage current at series resistance, q is Electron charge, R_T specifies thermal resistance, R_{sh} specifies the Shunt Resistor, R_s specifies Series Resistor, I_{sh} specifies shunt current, k specifies Boltzmann constant, and I_d specifies diode current.

The design structure can be used to calculate the PV cell array's total current output as follows:

$$I = N_p I_{PV} - N_p \frac{V_{PV} + I_{PV} R_s}{R_{sh}} - N_p I_s\left[\exp\left(\frac{qR_T}{akT}\right) - 1\right] \quad (3)$$

This allows for the temperature-dependent variation of the reserved saturation current to be calculated,

$$I_s = e^{\left[\frac{q}{nk}\left(\frac{1}{T_{op}} - \frac{1}{T_{ref}}\right)\right]} I_{rs}\left(\frac{T_{op}}{T_{ref}}\right)^3 \quad (4)$$

where, T_{op} defines Temperature at operating point, T_{ref} specifies reference temperature at rated value.

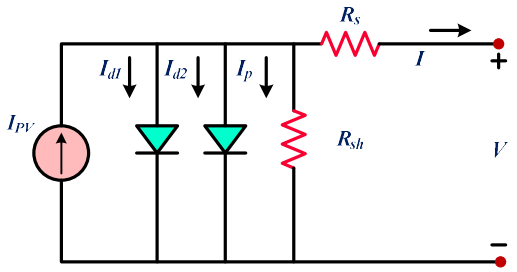

Fig.1: Equivalent Circuit of PV cell

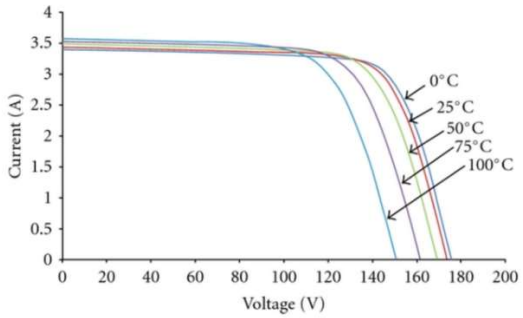

Fig.2: I-V characteristics of Solar cell

Subsequently, the MPPT controller adjusts the switching device in the converter architecture based on the variations in irradiance levels at each time instant.

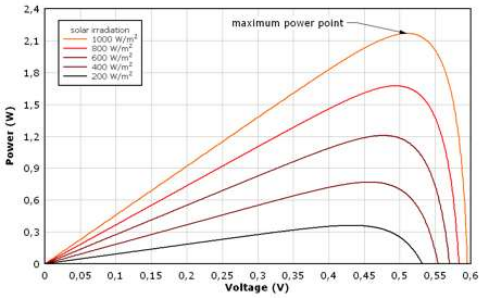

Fig.3: P-V characteristics of Solar cell

Important characteristics of solar cells include the fill factor, maximum power point (MPP), open circuit voltage (Voc), short circuit current (Isc), and solar cell efficiency. Isc stands for the current in the event of a short circuit, which happens at zero voltage and low impedance.

$$I(at\ V = 0) = I_{sc} \quad (5)$$

where Isc is found in the power quadrant's greatest current value and near the start of the forward-bias sweep. In a perfect world, the maximum current value is equal to the entire current that photon excitation causes in the solar cell.

$$C(at\ I = 0) = V_{OC} \quad (6)$$

where VOC, for a forward-bias sweep, is also the highest voltage differential across the cell in the energy quadrant. In the quadrant where power is biasedly forwarded, Voc equals Vm. The open circuit voltage is expressed as follows:

$$V_{OC} = \frac{AkT_c}{q} \ln \frac{I_{pv}}{I_s} \quad (7)$$

where Tc is the cell operating temperature (ºK), A is the ideality constant of the diode, Ipv is the saturation or leakage current of the diode, and q is the electron charge [1.60 x 10-19ºC]. k is the Boltzmann constant [1.38 x 10-23J/K].

$$P_m = V_m * I_m \quad (8)$$

Im stands for the maximum current. The relationship between a solar cell's maximum power output and the power of incident light is known as its efficiency.

$$\eta = \frac{P_m}{P_{in}} \quad (9)$$

where Pin is the input power from source.

$$Pin = G.AC \quad (10)$$

The fill factor (FF) is worked out as follows:

$$FF = \frac{P_m}{V_{oc} I_{sc}} \quad (11)$$

Fill factors typically fall between 0.5 and 0.82. But when the temperature of the cell rises, the fill factor falls.

5.1 Nonlinear Model for VSI Using an LCL Filter

In this part, the dynamic equation of the Voltage Source Inverter (VSI) with the LCL filter is simulated. Actual (P) and reactive (Q) power are taken into consideration within the Place of Common Coupling (PCC) bus together with other unmodeled dynamic characteristics. Using the ABC to dq conversion equations reduces computing cost and eliminates unnecessary Phase-Locked Loop (PLL) variable estimates. The state-space model of the VSI with the LCL filter is described, and the dynamical framework can be stated in terms of power (P, Q). The LCL filter circuit simulation with damping resistance is shown in Figure 5, and the related equations are as follows.

$$I^{*}_{i,abc} = \frac{\left(V_{i,abc} - V_{1,abc}\right)}{L_1} - \frac{R_1}{L_1}\left(I_{i,abc}\right) \quad (12)$$

$$I^{*}_{1,abc} = \frac{\left(V_{1,abc} - V_{2,abc}\right)}{L_2} - \frac{R_2}{L_2}\left(I_{i,abc}\right) \quad (13)$$

$$V^{*}_{1,abc} = \frac{1}{C_1}\left(I_{i,abc} - I_{1,abc}\right) \quad (14)$$

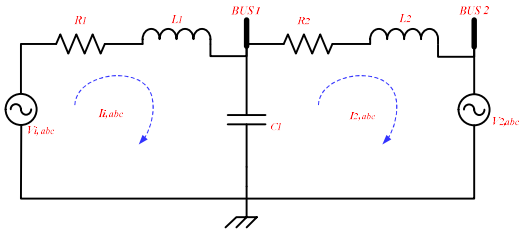

Fig 4: LCL filter circuit model with damping resistance

The real (P) and reactive (Q) power at buses 1 and 2 are calculated using the following equations:

$$P = v_{a1}\, i_{ai} + v_{b1}\, i_{bi} + v_{c1}\, i_{ci} \quad (15)$$

$$Q = \frac{\begin{bmatrix} v_{a1}\left(i_{bi} - i_{ci}\right) \\ + v_{b1}\left(i_{ci} - i_{ai}\right) \\ + v_{c1}\left(i_{ai} - i_{bi}\right) \end{bmatrix}}{\sqrt{3}} \quad (16)$$

The current parameters are formulated as follows:

$$\frac{d\, i_{id}}{dt} = -\frac{R_1}{L_1} i_{di} + i\omega_{qi} + \frac{\left(v_{di} - v_{d1}\right)}{L_1} \quad (17)$$

$$\frac{d\, i_{iq}}{dt} = -\frac{R_1}{L_1} i_{qi} + i\omega_{di} + \frac{\left(v_{qi} - v_{q1}\right)}{L_1} \quad (18)$$

The active and reactive power output in bus 1 is expressed as:

$$P = \left(v_{d1}\, i_{di} + v_{q1}\, i_{qi}\right) \quad (19)$$

$$Q = \left(v_{q1}\, i_{di} + v_{d1}\, i_{qi}\right) \quad (20)$$

$$\frac{dP}{dt} = -\frac{1}{L_1} R_1 P - \omega Q + \frac{1}{L_1} u_q \quad (21)$$

$$\frac{dQ}{dt} = -\frac{1}{L_1} R_1 Q + \omega P + \frac{1}{L_1} u_p \quad (22)$$

In order to determine bus 2's reactive and real power, the control variables are stated as follows,

$$u_p = v_{q1}\, v_{di} - v_{d1}\, v_{qi} \quad (23)$$

$$u_q = v_{d1}\, v_{di} + v_{q1}\, v_{qi} - \left(v^2_{d1} + v^2_{q1}\right) \quad (24)$$

In the part that follows, the MPPT problem and power flow control strategy based on the suggested hybrid technique are then thoroughly detailed.

5.2 Application of Proposed Hybrid Technique for MPPT and PFM

The aim of choosing the RFA and OA for maximizing power extraction in a solar PV module is to improve prediction accuracy and optimization efficiency. RFA's ensemble learning technique enhances the accuracy of solar power predictions by managing large datasets and capturing complex interactions. OA, a nature-inspired optimization algorithm, effectively identifies the maximum power point under varying conditions. Together, these algorithms ensure precise and adaptive control of the PV system, leading to optimal power extraction, increased energy efficiency, and reduced operational costs, ultimately promoting sustainable and reliable solar energy utilization.

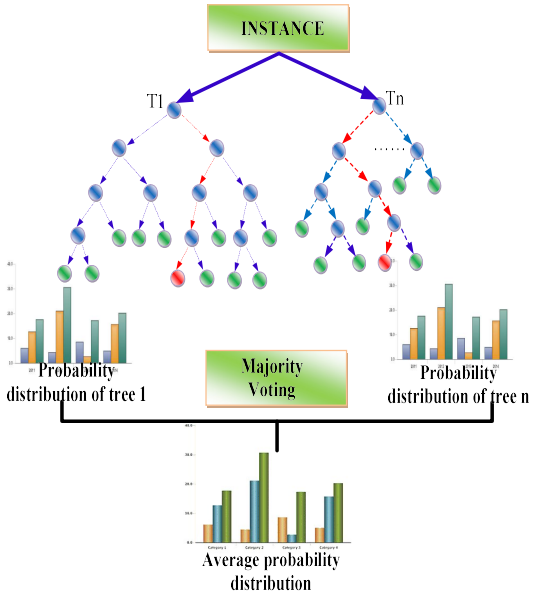

Fig 5: Structure of RFA technique

This section describes how hybrid technology can be used to provide consistent load capacity by integrating a photovoltaic generating system with an energy storage system. The RFA and OA are combined in the suggested hybrid approach, known as RFA-OA [29, 30]. This study's major goal is to track the MPP as efficiently as possible while keeping the power flowing within the grid-connected HRES. In order to account for fluctuations in power, the RFA-OA technique further forecasts control signals for the VSI on the load side. The suggested techniques enable the prediction of control parameters such load-side power demand, storage element state of charge, and RES accessibility. Fig. 6 depicts the RFA technique's structure.

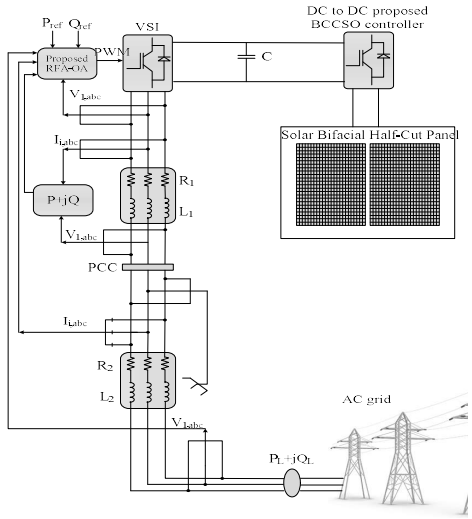

Fig. 6. Architecture of solar bifacial half cut single PV panel generating system

The system data for the proposed study, matrix D, include real and reactive power controller gain settings and

$$D=\begin{bmatrix} G_p^{11}(t)G_p^{11}(t) & G_p^{12}(t)G_p^{12}(t) & \dots & G_p^{1n}(t)G_p^{1n}(t) \\ G_p^{21}(t)G_p^{21}(t) & G_p^{22}(t)G_p^{22}(t) & \dots & G_p^{2n}(t)G_p^{2n}(t) \\ \vdots & \vdots & \vdots & \vdots \\ G_p^{m1}(t)G_p^{m1}(t) & G_p^{m2}(t)G_p^{m2}(t) & \dots & G_p^{mn}(t)G_p^{mn}(t) \end{bmatrix} \quad (25)$$

The following formula is used to determine each osprey's fitness based on its initial position values:

$$f=\begin{bmatrix} f_1[(G_p^{11}(t)G_p^{11}(t) & \cdots & \cdots & G_p^{1n}(t)G_p^{1n}(t))] \\ f_2[(G_p^{21}(t)G_p^{21}(t) & \cdots & \cdots & G_p^{2n}(t)G_p^{2n}(t))] \\ \vdots & & \vdots & \vdots \\ f_n[(G_p^{m1}(t)G_p^{m1}(t) & \cdots & \cdots & G_p^{mn}(t)G_p^{mn}(t))] \end{bmatrix} \quad (26)$$

Equation (27), which examines the objective function in the optimisation issue is represented by minimising the error value.

$$Obj\ \ F_j = Min\ \ E(x) \quad (27)$$

$$E(x)= p_{ref}(t)- p_1(t), E(x)= q_{ref}(t)- q_1(t),$$

the error function of the system is represented as $E(x)$.

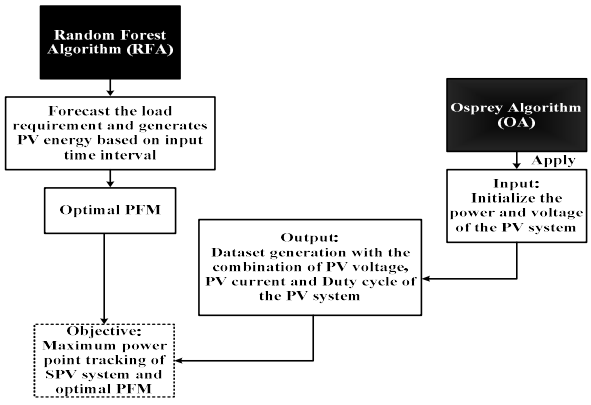

Fig. 7. Flow diagram of Proposed Technique

At system starting, the algorithm is set up to control the HRES system's power flow, resulting in the best MPPT at the end of this stage. The RFA is specifically made for the solar photovoltaic system's MPPT. By properly satisfying load requirements, this control technique effectively minimises fluctuations in system characteristics and external disturbances. To find online control signals, the RFA technique executes the active and reactive power difference concurrently. RFA functions during the prediction process as an ensemble machine learning technique. The total number of trees in the forest and the number of splits in the subset at each node are the two hyperparameters that are included. Fig. 7 displays the proposed technique's flow diagram.

6 Results and discussion

The suggested hybrid technique's efficacy is assessed by contrasting its results with three widely used MPPT techniques: Grey Wolf Optimization (GWO), Genetic Algorithm-Fuzzy (GAFUZZY), and the base (traditional) method. The following tests are performed on all four algorithms: The first case involves a continuous change in irradiance, the second involves a sudden step change in irradiance, the third involves simultaneous step changes in irradiance, and the fourth case involves partial shading.

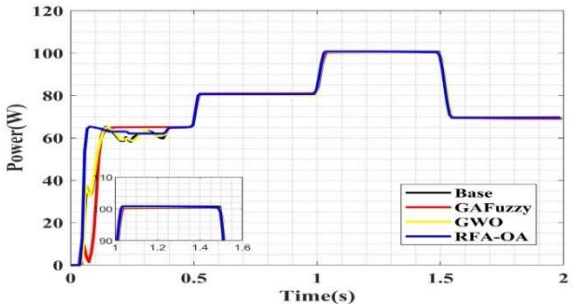

Fig. 8. PV power comparison under case 1

The power of the suggested and current approaches is shown in Fig. 8. In the recommended method, the power value increases to 60W at intervals of 0.1 to 0.5 seconds. On the other hand, for the methods that are currently in use (Base, GAFUZZY, and GWO), the power drops to 100W after 1.5 seconds.

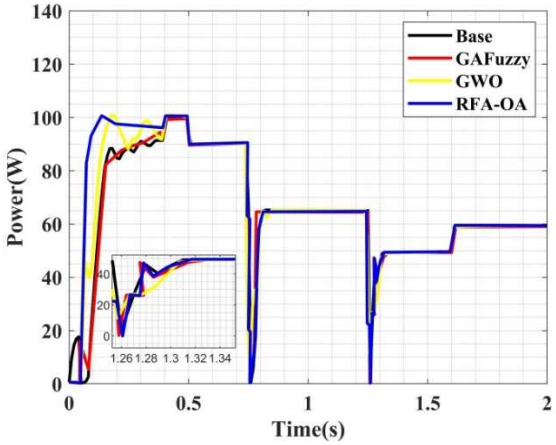

Fig.9. PV power comparison under case 2

Fig.9 shows a comparison of PV power between the suggested and current methods. The current methods taken into consideration include Base, GAFUZZY, and GWO. There is a time span of 0 to 2 seconds. The PV

power in the suggested method is more than in the methods already in use.

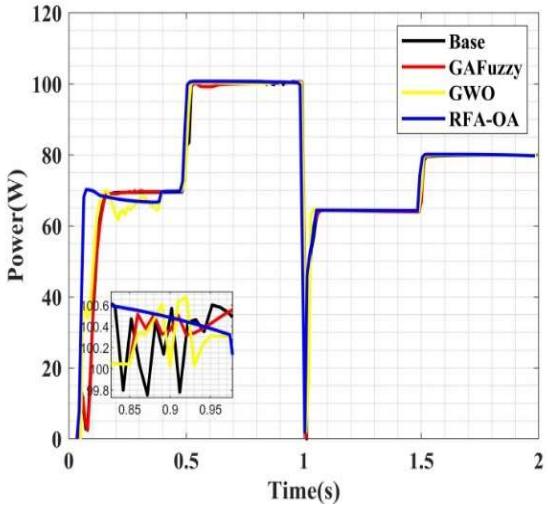

Fig.10. PV power comparison under case 3

PV power is compared between the proposed and existing technologies in Fig. 10. In this subplot, the usefulness of the recommended approach is investigated. The current methods taken into consideration include Base, GAFUZZY, and GWO. In the time intervals of 0 to 2 seconds, the suggested technique shows higher values than the current techniques.

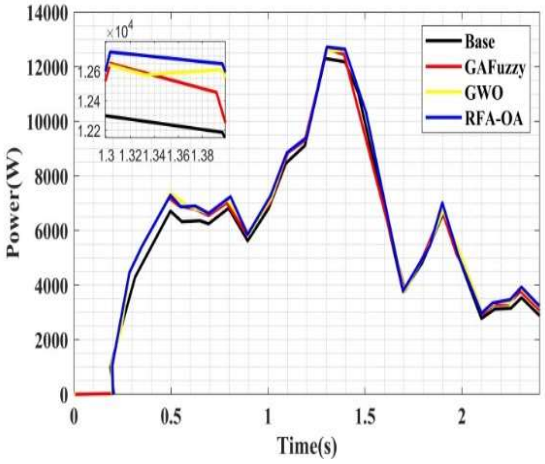

Fig. 11. PV power comparison under case 4

The output power produced by solar systems utilizing the SSA-GBDT approach is compared to earlier methods such as GBDT, ANN, and SSA in Fig. 11. The purpose of the analysis is to evaluate the effectiveness of different approaches versus the established method in generating PV output power under partial shadowing. In this analysis, the output power generated by the SSA-GBDT algorithm surpasses 12000 W, outperforming the output power generated by the ANN, GBDT, and SSA algorithms combined. Fig.11's left side displays a zoomed in view of the output power produced by the PV's SSA-GBDT, SSA, GBDT, and ANN under partial shadowing.

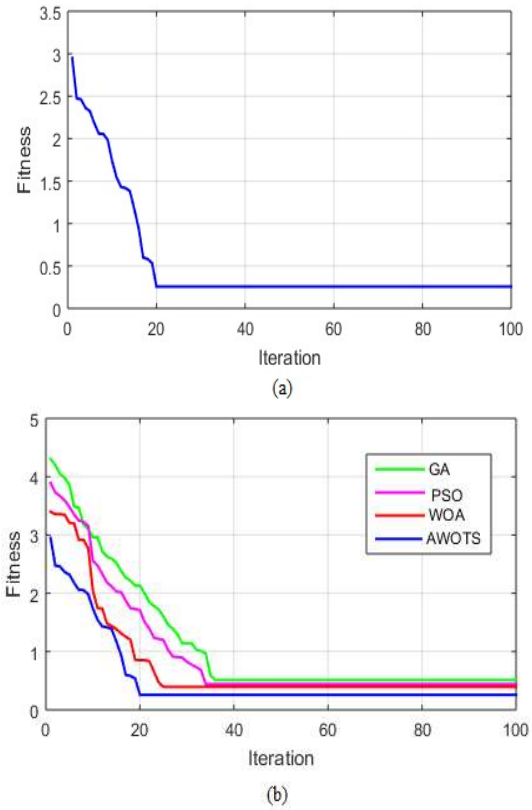

Fig. 12. Analysis of (a) Fitness of proposed technique (b) Fitness Comparison

The fitness graph of the suggested methodology is shown in Figure 12, along with a comparison of its fitness over several iterations with other methods. The fitness analysis of the suggested technique is shown in Figure 12(a), where fitness values ranging from 3 to 0.3 indicate convergence at the 20th iteration. The suggested method and current methods are compared for fitness in Figure 12(b). The suggested approach achieves fitness values between 3 and 0.3 at the 20th iteration, when it converges. Meanwhile, the Grey Wolf Optimization (GWO) converges at the 24th iteration, yielding fitness values from 3.4 to 0.4. The Genetic Algorithm with Fuzzy Logic (GA-Fuzzy) converges at the 36th iteration, producing fitness values from 3.5 to 0.5. Finally, the base method converges at the 38th iteration, with fitness values ranging from 4.2 to 0.6.

Table 1. Efficiency comparison of source power

Efficiency of PV power (%)	
Solution techniques	**Source**
	PV panel
ANN [31]	79.265
GBDT [31]	82.237
SSA [31]	98.935
SSA-GBDT [31]	99.710
Proposed Technique	99.951

The efficiency comparison of PV power between the suggested and current methods is shown in Table 1. The suggested method's effectiveness in every scenario, which produces the best efficiency outcomes, is well demonstrated in the table. Efficiency shows that the chosen approach optimizes power extraction from the photovoltaic system.

Table 2: Modeling metrics under various trials

Metrics	50 trails			
	Base	**GAFuzzy**	**GWO**	**Proposed**
RMSE	25.3	17.8	22.4	7.710
MAPE	16.1	5.3	12.1	0.732
MBE	6.1	1.8	4.1	0.9955
Execution time (s)	6.7	5.4	7.0	1.009
	100 trails			
RMSE	28.4	22.9	25.5	5.07
MAPE	17.2	6.4	15.0	0.90
MBE	11.1	6.9	7.1	1.64
Execution time (s)	9	8	7.3	2

For both the suggested and current approaches, Table 2 shows the MAPE (Mean Absolute Percentage Error), RMSE (Root Mean Squared Error), MBE (Mean Bias Error), and execution time. For the proposed method, the RMSE is 7.710, MAPE is 0.732, MBE is 0.9955, and execution time is 1.009. In 100 trials, the proposed method yields an RMSE of 5.07, MAPE of 0.90, MBE of 1.64, and an execution time of 2s.

In the first case of continuous change in irradiance, the system smoothly adapts to varying light levels, ensuring steady power extraction. In the second case of a sudden step change in irradiance, the system quickly adjusts to the new light conditions, demonstrating its responsiveness. The third case, with simultaneous step changes in irradiance, tests the system's ability to handle multiple rapid adjustments, showing its robustness. In the fourth case involving partial shading, the system effectively manages uneven light distribution, optimizing power extraction despite the challenges. Overall, these scenarios validate the system's adaptability and efficiency under diverse conditions.

7 Conclusion

Challenges in maximizing power extraction in a solar PV module include varying irradiance levels, partial shading, temperature fluctuations, and the need for real-time optimization. Additionally, accurately predicting and responding to rapid environmental changes requires sophisticated algorithms, robust hardware, and efficient energy management systems.This work proposes an efficient RFA-OA technique to enhance the MPPT and power flow control of a solar PV production system. For the DC-DC converter of the SPV, the RFA-OA technique determines the required duty cycles under instantaneous shading conditions. The RFA algorithm is used to properly design the MPPT of the SPV system. This control method meets load requirements as efficiently as possible while minimising changes in system characteristics and external disturbances. The recommended method is carried out using the MATLAB/Simulink platform. The simulation's findings demonstrate that the hybrid solution that has been recommended effectively tracks the PV generating system's maximum power production and surpasses existing methods for power flow management in solar PV generation systems. Future directions for maximizing power extraction in solar PV modules include advancements in machine learning algorithms, integration of real-time adaptive control systems, and development of more efficient MPPT techniques, enhanced energy storage solutions, and improved PV materials to increase efficiency and resilience under varying environmental conditions.

References

1. W. Zhou, C. Lou, Z. Li, L. Lu and H. Yang, "Current status of research on optimum sizing of stand-alone hybrid solar–wind power generation systems", Applied Energy, vol. 87, no. 2, pp. 380-389, (2010).
2. I. Syed, "Near-optimal standalone hybrid PV/WE system sizing method", Solar Energy, vol. 157, pp. 727-734, (2017).
3. R. Maouedj, A. Mammeri, M. Draou and B. Benyoucef, "Techno-economic Analysis of a Standalone Hybrid Photovoltaic-wind System. Application in Electrification of a House in Adrar Region", Energy Procedia, vol. 74, pp. 1192-1204, (2015).
4. M. Ismail, M. Moghavvemi, T. Mahlia, K. Muttaqi and S. Moghavvemi, "Effective utilization of excess energy in standalone hybrid renewable energy systems for improving comfort ability and reducing cost of energy: A review and analysis", Renewable and Sustainable Energy Reviews, vol. 42, pp. 726-734, (2015).
5. S. Aissou, D. Rekioua, N. Mezzai, T. Rekioua and S. Bacha, "Modeling and control of hybrid photovoltaic wind power system with battery storage", Energy Conversion and Management, vol. 89, pp. 615-625, (2015).
6. T. Alnejaili, S. Drid, D. Mehdi, L. Chrifi-Alaoui, R. Belarbi and A. Hamdouni, "Dynamic control and advanced load management of a stand-alone hybrid renewable power system for remote housing", Energy Conversion and Management, vol. 105, pp. 377-392, (2015).
7. T. Ma, H. Yang, L. Lu and J. Peng, "Pumped storage-based standalone photovoltaic power generation system: Modeling and techno-economic optimization", Applied Energy, vol. 137, pp. 649-659, (2015).
8. R. Gupta, R. Kumar and A. Bansal, "BBO-based small autonomous hybrid power system optimization incorporating wind speed and solar radiation forecasting", Renewable and Sustainable Energy Reviews, vol. 41, pp. 1366-1375, (2015).
9. B. Bilal, V. Sambou, P. Ndiaye, C. Kébé and M. Ndongo, "Study of the Influence of Load Profile Variation on the Optimal Sizing of a Standalone Hybrid PV/Wind/Battery/Diesel System", Energy Procedia, vol. 36, pp. 1265-1275, (2013).
10. B. Bilal, V. Sambou, C. Kébé, P. Ndiaye and M. Ndongo, "Methodology to Size an Optimal Stand-

Alone PV/wind/diesel/battery System Minimizing the Levelized cost of Energy and the CO2 Emissions", Energy Procedia, vol. 14, pp. 1636-1647, (2012).

11. M. Dali, J. Belhadj and X. Roboam, "Hybrid solar–wind system with battery storage operating in grid-connected and standalone mode: Control and energy management – Experimental investigation", Energy, vol. 35, no. 6, pp. 2587-2595, (2010).
12. T. Khatib, I. Ibrahim and A. Mohamed, "A review on sizing methodologies of photovoltaic array and storage battery in a standalone photovoltaic system", Energy Conversion and Management, vol. 120, pp. 430-448, (2016).
13. R. Kamel, "New inverter control for balancing standalone micro-grid phase voltages: A review on MG power quality improvement", Renewable and Sustainable Energy Reviews, vol. 63, pp. 520-532, (2016).
14. A. Maheri, "Multi-objective design optimization of standalone hybrid wind-PV-diesel systems under uncertainties", Renewable Energy, vol. 66, pp. 650-661, (2014).
15. A. Maheri, "A critical evaluation of deterministic methods in size optimization of reliable and cost effective standalone hybrid renewable energy systems", Reliability Engineering & System Safety, vol. 130, pp. 159-174, (2014).
16. T. Ma, H. Yang and L. Lu, "A feasibility study of a stand-alone hybrid solar–wind–battery system for a remote island", Applied Energy, vol. 121, pp. 149-158, (2014).
17. S. Ahmadi and S. Abdi, "Application of the Hybrid Big Bang–Big Crunch algorithm for optimal sizing of a stand-alone hybrid PV/wind/battery system", Solar Energy, vol. 134, pp. 366-374, (2016).
18. A. Perera, R. Attalage, K. Perera and V. Dassanayake, "Designing standalone hybrid energy systems minimizing initial investment, life cycle cost and pollutant emission", Energy, vol. 54, pp. 220-230, (2013).
19. H. Belmili, M. Almi, B.Bendib and S. Bolouma, "A Computer Program Development for Sizing Stand-alone Photovoltaic-Wind Hybrid Systems", Energy Procedia, vol. 36, pp. 546-557, (2013).
20. S. Semaoui, A. Arab, S. Bacha and B. Azoui, "Optimal Sizing of a Stand-alone Photovoltaic System with Energy Management in Isolated Areas", Energy Procedia, vol. 36, pp. 358-368, (2013).
21. Ibrahim, A.W., Zhijian, F., Jiuqing, C., Farh, H.M.H., Aboudrar, I., Dagal, I., Kandil, T., Al-Shamma'a, A.A. and Saeed, F. Fast DC-link voltage control based on power flow management using linear ADRC combined with hybrid salp particle swarm algorithm for PV/wind energy conversion system. International Journal of Hydrogen Energy, 61, pp.688-709 (2024).
22. Versaci, M. and La Foresta, F. Fuzzy Approach for Managing Renewable Energy Flows for DC-Microgrid with Composite PV-WT Generators and Energy Storage System. Energies, 17(2), p.402 (2024).
23. Jamadar, S. and Singaram, G. Design and development of energy management system for solar electric vehicle with dynamic power split approach. Australian Journal of Electrical and Electronics Engineering, pp.1-12 (2024).
24. Michael, A.A., Kehinde, O.P., Olawale, O.B., Adebayo, O.E. and Samuel, A.O. Dynamic Impact of Hybrid Wind-Solar Photovoltaic Power Injection on Small Signal Stability of Nigerian 11 kV Power System using Self Organizing Map Neural Network. Scientific African, p.e02214 (2024).
25. Elymany, M.M., Enany, M.A. and Elsonbaty, N.A., 2024. Hybrid optimized-ANFIS based MPPT for hybrid microgrid using zebra optimization algorithm and artificial gorilla troops optimizer. Energy Conversion and Management, 299, p.117809.
26. Maka, A.O. and Chaudhary, T.N., 2024. Performance investigation of solar photovoltaic systems integrated with battery energy storage. Journal of Energy Storage, 84, p.110784.
27. Endiz, M.S., 2024. Design and implementation of microcontroller-based solar charge controller using modified incremental conductance MPPT algorithm. Journal of Radiation Research and Applied Sciences, 17(2), p.100938.
28. Aljafari, B., Balachandran, P.K., Samithas, D. and Thanikanti, S.B., 2023. Solar photovoltaic converter controller using opposition-based reinforcement learning with butterfly optimization algorithm under partial shading conditions. Environmental Science and Pollution Research, 30(28), pp.72617-72640.
29. Oliver, J.S., David, P.W., Balachandran, P.K. and Mihet-Popa, L., 2022. Analysis of grid-interactive PV-fed BLDC pump using optimized MPPT in DC–DC converters. Sustainability, 14(12), p.7205.
30. Dehghani, M. and Trojovský, P., 2023. Osprey optimization algorithm: A new bio-inspired metaheuristic algorithm for solving engineering optimization problems. Frontiers in Mechanical Engineering, 8, p.1126450.
31. Ganti, P.K., Naik, H. and Barada, M.K., 2022. Environmental impact analysis and enhancement of factors affecting the photovoltaic (PV) energy utilization in mining industry by sparrow search optimization based gradient boosting decision tree approach. Energy, 244, p.122561.